



ISSN (Print) : 2320 – 3765
ISSN (Online): 2278 – 8875

International Journal of Advanced Research in Electrical, Electronics and Instrumentation Engineering

(An ISO 3297: 2007 Certified Organization)

Vol. 5, Special Issue 8, November 2016

Particle Swarm Optimization Based Feedback Controller Design for Induction Motor Soft-Starting

A. Chandra Sekhar¹, Dr. N. Bhoopal²

Assistant Professor, Department of Electrical and Electronics Engineering, B.V. RAJU Institute of Technology,
Narsapur, India¹

Professor & Head of the Department, Department of Electrical and Electronics Engineering, B.V. RAJU Institute
of Technology, Narsapur, India²

ABSTRACT: The objective of this work is to design and implement a closed loop system for induction motor starting at rated current. Thyristorized AC voltage regulator is used as the starting equipment and motor current regulation is carried out using an optimally tuned Proportional-Integral (PI) controller. Since, AC voltage controller fed starting of induction motor is a non-linear process, identification of optimal values of PI controller constants is performed using Particle Swarm Optimization (PSO). The complete drive system including AC voltage controller fed induction motor in conjunction with optimal PI controller is first simulated in MATLAB and subsequently verified experimentally. The successful implementation with a low cost microcontroller illustrates the feasibility of the new approach.

KEYWORDS: Soft starter, Induction Motor, PSO.

Nomenclature

V_{ds}	Direct axis component of stator voltage
V_{qs}	Quadrature axis component of stator voltage
i_{ds}	Direct axis component of stator current
i_{qs}	Quadrature axis component of stator current
i_{dr}	Direct axis component of rotor current
i_{qr}	Quadrature axis component of rotor current
i_r, i_y, i_b	Motor phase currents
r_s	Stator winding resistance
r_r	Rotor winding resistance
L_m	Magnetizing inductance
L_s	Stator winding inductance
L_r	Rotor winding inductance
ω_r	Motor speed in rad/sec
T_e	Electromagnetic torque
T_L	Load torque
P	Number of poles
J	Moment of Inertia of the motor
α	Firing angle
I_r	Actual motor current
I_r^*	Rated motor current
e	Error
α_0	Initial firing angle
K_p	Proportional gain
K_I	Integral gain

International Journal of Advanced Research in Electrical, Electronics and Instrumentation Engineering

(An ISO 3297: 2007 Certified Organization)

Vol. 5, Special Issue 8, November 2016

I. INTRODUCTION

The methods of starting of three-phase induction motors are generally classified into four basic categories [1]: direct online starting, electromechanical reduced voltage starting, solid-state reduced voltage starting and variable-frequency-drive (VFD) starting. The cheapest way is direct online starting, but the major disadvantage is large initial current surge leading to voltage dips in the supply system. Electromechanical reduced-voltage starting comprises auto-transformer starting, star/delta starting and resistor/reactor starting. Among these, star/delta starting is more popular since it is cheap, compact and causes no power loss. However this method can be applied only for normally delta-connected stator provided with six leads. Conventional starting elements require some type of mechanical switch or contact and have several drawbacks [2, 3], such as need for frequent inspection and maintenance, non-simultaneous switching of motor phases to the supply, failure in the moving parts due to large amount of switching etc.

Availability of high-power devices has led to the development of solid state starters replacing conventional starters. An earlier work in this direction is seen in [4, 5]. The solid state starter consisted of a pair of back-to-back connected SCRs and the firing angle of SCRs was varied to control rate of change of KVA with respect to time. Such a scheme is examined for pulp and paper industry in [6]. A solid state voltage contactor employing anti-parallel SCRs is given in [7]. The concept of use of SCR voltage regulator with firing angle control for smooth induction motor starting is labeled as “soft starter” and a closed loop soft starter with fuzzy logic controller is available in [8]. A closed loop optimal soft starting of ac voltage controller fed induction motor drive based on voltage across the thyristor is seen in [9]. While earlier works were confined to current limit starting, performance enhancement of starting torque is profile was later addressed [10, 11]. Numerical solution method is attempted in [10] for improved starting current and torque profile whereas the method suggested in [11] consists of two parts: a linear initial firing angle scheme which eliminates starting torque ripples and a current control strategy which consists of successive co-sinusoidal and constant function segments of triggering angle of SCRs. A soft starter with voltage and power factor angle as feedback signals is given in [12], whereas starting torque optimization is carried out in [13]. The work in [14] explains the use of Artificial Neural Network (ANN) for the generation of SCR firing angles for soft starting. Soft starters are also employed for energy saving too [15, 16]. The works in [17, 18] indicate that soft starters are increasingly employed in industries nowadays. While the schemes in [4-7] are of open loop type, the soft starters in [8-14] work in closed loop mode. It is important to mention that the closed loop control strategies are generally obtained by repeatedly simulating the motor model several times and employing trial and error based approach.

While the soft-starter has been increasingly employed in the industries now-a-days, the design procedure of feedback controller for rated current starting is not available in literature. This is important in particular because, AC voltage controller fed induction motor drive system is described by a fifth order differential equation and is highly non-linear during starting due to continuous and large variation of motor speed. This demands a detailed design and implementation of a feedback controller for soft-starter fed induction motor drive. In this context, the feedback controller design is formulated as an optimization problem and the solution is achieved to obtain good dynamic response.

This paper formulates an optimization model for the soft starter and the solution is achieved through Particle Swarm Optimization (PSO) [19-23]. Thyristorized AC voltage controller is proposed to work in a closed loop mode with a Proportional-Integral (PI) controller for regulating the motor current at its rated value during starting. The control constants of the PI controller are obtained through PSO. For this, the soft-starter fed induction motor drive together with PI controller is developed in MATLAB and subsequently a suitable objective function is tailored for the estimation of optimal values of PI controller constants using PSO. Extensive simulation results supported with experimental waveforms are provided to validate the proposed method.

II. PARTICLE SWARM OPTIMIZATION FOR PI CONTROLLER DESIGN

(A) Formulation of the problem

The schematic of induction motor soft starting is depicted in figure 1. Here, motor model is described by the fifth order differential equation [23] and is given below:

The stator voltages, V_{qs} and V_{ds} are given by,

International Journal of Advanced Research in Electrical, Electronics and Instrumentation Engineering

(An ISO 3297: 2007 Certified Organization)

Vol. 5, Special Issue 8, November 2016

$$\begin{bmatrix} V_{qs} \\ V_{ds} \end{bmatrix} = \begin{bmatrix} 1 & 0 & 0 \\ 0 & \frac{-1}{\sqrt{3}} & \frac{1}{\sqrt{3}} \end{bmatrix} \begin{bmatrix} V_{rs} \\ V_{ys} \\ V_{bs} \end{bmatrix} \dots\dots\dots (1)$$

where V_{rs} , V_{ys} and V_{bs} are motor terminal voltages and are derived below:

With AC voltage controller as the power electronic interface between the AC supply and induction motor, variation of SCR firing angle, α changes motor stator voltage. This component is now introduced and the motor stator voltage is described below.

Assuming the instantaneous phase voltages as

$$V_r = V_m \sin(\omega t) \dots\dots\dots (2)$$

$$V_y = V_m \sin(\omega t - 2\pi/3) \dots\dots\dots (3)$$

$$V_b = V_m \sin(\omega t + 2\pi/3) \dots\dots\dots (4)$$

With the SCR voltage controller between supply phase voltage and motor phase windings, the motor phase voltage is given by

$$\left. \begin{aligned} V_r &= V_m \sin(\omega t), && \text{when } i_r \neq \text{zero and } \omega t < \alpha, \\ &= e_r && \text{when } i_r = \text{zero and } \omega t < \alpha, \\ &= V_m \sin(\omega t), && \text{when } i_r \neq \text{zero and } \omega t \geq \alpha. \end{aligned} \right\} \dots\dots\dots (5)$$

Similarly

$$\left. \begin{aligned} V_y &= V_m \sin(\omega t - \frac{2\pi}{3}), && \text{when } i_y \neq \text{zero and } \omega t < \alpha, \\ &= e_y && \text{when } i_y = \text{zero and } \omega t < \alpha, \\ &= V_m \sin(\omega t - \frac{2\pi}{3}), && \text{when } i_y \neq \text{zero and } \omega t \geq \alpha. \end{aligned} \right\} \dots\dots\dots (6)$$

$$\left. \begin{aligned} V_b &= V_m \sin(\omega t + \frac{2\pi}{3}), && \text{when } i_b \neq \text{zero and } \omega t < \alpha, \\ &= e_b && \text{when } i_b = \text{zero and } \omega t < \alpha, \\ &= V_m \sin(\omega t + \frac{2\pi}{3}), && \text{when } i_b \neq \text{zero and } \omega t \geq \alpha. \end{aligned} \right\} \dots\dots\dots (7)$$

For SCR voltage controller with three wire system, there exists neutral shift voltage given by:

$$V_{sn} = \frac{1}{3} * (V_r + V_y + V_b) \dots\dots\dots (8)$$

Thus the three-phase forcing voltages at the machine terminals are given by:

$$\left. \begin{aligned} V_{rs} &= V_r - V_{sn} \\ V_{ys} &= V_y - V_{sn} \\ V_{bs} &= V_b - V_{sn} \end{aligned} \right\} \dots\dots\dots (9)$$

Equations (2) to (9) completely describe the dynamic of AC voltage controller fed induction motor drive, where SCR firing angle, α and load torque T_L are independent variables. A dedicated computer program is now developed in MATLAB for transient response analysis of induction motor drive. The parameters of induction motor are listed in Appendix.

International Journal of Advanced Research in Electrical, Electronics and Instrumentation Engineering

(An ISO 3297: 2007 Certified Organization)

Vol. 5, Special Issue 8, November 2016

The induced emfs in each phase are given below:

$$\begin{bmatrix} e_r \\ e_y \\ e_b \end{bmatrix} = \sqrt{\frac{2}{3}} \begin{bmatrix} 1 & 0 \\ -\frac{1}{2} & \frac{\sqrt{3}}{2} \\ \frac{1}{2} & -\frac{\sqrt{3}}{2} \end{bmatrix} \begin{bmatrix} e_{dr} \\ e_{qr} \end{bmatrix} \quad (10)$$

The back emfs in $d - q$ axis of the motor are given by,

$$\begin{bmatrix} e_{dr} \\ e_{qr} \end{bmatrix} = \omega_r \begin{bmatrix} l_{rl} i_{qr} + \psi_q \\ l_{rl} i_{qr} + \psi_d \end{bmatrix} \quad (11)$$

where,
$$\begin{bmatrix} \psi_d \\ \psi_q \end{bmatrix} = \begin{bmatrix} \psi_{dr} - l_{rl} i_{qr} \\ \psi_{qr} - l_{rl} i_{qr} \end{bmatrix} \quad (12)$$

The rotor flux linkages in the $d - q$ axis ψ_{dr} and ψ_{qr} are given by,

$$\begin{bmatrix} \psi_{dr} \\ \psi_{qr} \end{bmatrix} = \begin{bmatrix} L_r & L_m & 0 & 0 \\ 0 & 0 & L_r & L_m \end{bmatrix} \begin{bmatrix} i_{ds} \\ i_{qs} \\ i_{dr} \\ i_{qr} \end{bmatrix} \quad (13)$$

The state space model of induction motor is given below:

$$\begin{bmatrix} V_{qs} \\ V_{ds} \\ 0 \\ 0 \end{bmatrix} = \begin{bmatrix} r_s + L_s p & 0 & L_m p & 0 \\ 0 & r_s + L_s p & 0 & L_m p \\ L_m p & -\omega_r L_m & r_r + L_r p & -\omega_r L_r \\ \omega_r L_m & L_m p & \omega_r L_r & r_r + L_r p \end{bmatrix} \begin{bmatrix} i_{qs} \\ i_{ds} \\ i_{qr} \\ i_{dr} \end{bmatrix} \quad (14)$$

Where, $p = \frac{d}{dt}$

The electromagnetic torque is given by,

$$T_e = \frac{3}{2} \frac{P}{2} L_m (i_{dr} i_{qs} - i_{qr} i_{ds}) \quad (15)$$

The rotor speed in rad/sec is governed by,

$$P \omega_r = \frac{T_e - T_L}{J} \quad (16)$$

The inputs to the motor model are SCR firing angle, α and load torque T_L . The motor is started on no-load i.e., $T_L = 0$ and the motor current, I_r evaluated through the model, is compared with rated motor current, I_r^* . The error is given to the PI controller, which calculates the change in firing angle, $\Delta\alpha$. The value of α_0 indicates initial SCR firing angle and is suitably selected.

International Journal of Advanced Research in Electrical, Electronics and Instrumentation Engineering

(An ISO 3297: 2007 Certified Organization)

Vol. 5, Special Issue 8, November 2016

In the block diagram shown in figure 1, the task is to identify optimum values of PI controller constants namely K_p and K_I such that motor current is kept constant at its rated value throughout starting. Let $e = I_r - I_r^*$ be the error and the objective here is to minimize the sum squared error.

This can be stated as an optimization problem and is given below:

Minimize,

$$F(\phi) = \sum_0^{t_s} (e(t))^2 \quad (17)$$

Subject to

$$\phi_{(lower)} \leq \phi \leq \phi_{(upper)} \quad \text{and} \quad 0 \leq \alpha \leq \pi$$

In the above,

t_s = Starting interval and

$\phi = \{K_p, K_I\}$ is the controller structure.

(B) PI controller design through Particle Swarm Optimization

The following steps describe how the PSO is designed and applied to the present problem. Various components of PSO such as *population*, *particle velocity*, *pbest*, *gbest* and *acceleration coefficients* as applied to the present work are illustrated.

Various steps of PSO are summarized in the following steps.

Step1. Generation of initial condition of each particle

Initial searching point X_{ij} and velocity V_{ij} of each particle is usually generated within the allowable range.

The current searching point is set to *pbest* for each particle. The best evaluated value of *pbest* is set to *gbest* and the position of particle with the best value is stored.

Step 2. Evaluation of searching point of each particle

The objective function value is calculated for each agent. If the value is better than the current *pbest* of the particle, the *pbest* value is replaced by the new value. If the best value of *pbest* is better than the current *gbest*, *gbest* is replaced by the best value and the particle with the best value is stored.

Step 3. Modification of each searching point

The new velocity term and position of i^{th} particle in j^{th} direction for $(k+1)^{th}$ iteration is given by equations (18) and (19):

$$V_{ij}^{k+1} = w.V_{ij}^k + c_1 \text{rand} () \times [pbest_{ij}^k - X_{ij}^k] + c_2 \text{rand} () \times [gbest_j^k - X_{ij}^k] \quad (18)$$

$$X_{ij}^{k+1} = X_j^k + V_{jk}^{k+1} \quad (19)$$

Step 4. Checking the terminating condition

When the current iteration number reaches the predetermined maximum iteration number, then exit.

Otherwise, go to step 2.

(C) Convergence graph

A dedicated computer program in MATLAB is developed for the estimation of PI controller constants for soft starting of induction motor through the above steps of PSO. The parameters of PSO such as number of particles, c_1 , and c_2 are used to achieve the optimal solution. The parameters used in the implementation of PSO are given in table-1.

International Journal of Advanced Research in Electrical, Electronics and Instrumentation Engineering

(An ISO 3297: 2007 Certified Organization)

Vol. 5, Special Issue 8, November 2016

Table 1. Parameters used in the implementation of GA

c_1	1.4
c_2	1.4
w_{\max}	0.9
w_{\min}	0.4
Population size	10
Termination criterion	100 iterations
Minimum value of K_p	0
Maximum value of K_p	10
Minimum value of K_i	0
Maximum value of K_i	10

The convergence characteristic curve is shown in figure 2. It is seen that the algorithm converges systematically to one of lowest values of objective function in a steady manner. It is important to mention that at each iterative step the least objective function is considered for plotting the convergence graph. The pace of initial convergence is very fast in the early stages of generations and as the optimization proceeds the rate of convergence decreases. At the end of 50 generations, the optimal values of controller parameters are obtained as follows:

$$K_p = 9.88 \quad \text{and} \quad K_i = 7.43$$

III. SIMULATED AND MEASURED RESULTS

Substitution of optimal controller constants in the closed loop block diagram of induction motor soft starting depicted in figure 1 will enable evaluation of start-up dynamics of the motor drive. In order to obtain experimental results also, a hardware set up for motor soft starting was fabricated in the laboratory and is shown in figure 4. Here, the power converter employed is a three-phase AC voltage regulator employing SCRs. The SCR firing angle is varied to adjust the stator voltage applied to the motor. The AC voltage controller consists of six SCRs labeled as $T_1, T_1', T_2, T_2', T_3$ and T_3' . The SCRs T_1 and T_1' are triggered at a delay of α and $\pi + \alpha$ respectively with reference to the zero crossing of R-phase voltage, V_{RN} . The SCRs T_2 and T_2' are triggered at a delay of $\frac{2\pi}{3} + \alpha$ and $\frac{2\pi}{3} + (\pi + \alpha)$ respectively. In a similar manner, the SCRs T_3 and T_3' are triggered at a delay of $\frac{4\pi}{3} + \alpha$ and $\frac{4\pi}{3} + (\pi + \alpha)$ respectively. The heart of the closed loop system is PIC16F876A micro controller which works as PI controller as well as firing pulse generator. The R-phase voltage, V_{RN} is stepped down and converted into a digital pulse using Zero Crossing Detection (ZCD) circuit and this pulse is fed to the pin RC_0 of the microcontroller. The microcontroller senses the status of this pin at each time and once zero crossing signal has come, it starts producing six firing pulses through RB0 to RB5 with a delay angle, α computed by the PI controller realized in the microcontroller.

Controller.

The dynamic motor model in figure 1 is now simulated for induction motor starting and the variation of few motor parameters are obtained and are shown in figure 5. Figure 5(a) shows motor terminal voltage and current during the starting process. It is seen that both the waveforms are distorted due to phase angle control action. Figure 5 (b) is the time variation of motor voltage and current at the end of soft starting. It obvious that phase angle control ceases at the end of motor starting and motor voltage and current become sinusoidal in shape with motor current magnitude falling to no load current value. Figure 5(c) depicts motor terminal voltage and current after the starting process is completed. The microcontroller based soft starter developed in the laboratory was used to start a three-phase induction motor and measured waveforms are included in figure 5. A good agreement is visible between measured and simulated values.

International Journal of Advanced Research in Electrical, Electronics and Instrumentation Engineering

(An ISO 3297: 2007 Certified Organization)

Vol. 5, Special Issue 8, November 2016

In order to confirm rated current start up, the time variation of rms value of motor terminal voltage and phase current are now computed and is shown in figure 6(a). It is clear that the motor current is almost constant at 2.7A during starting with adjustment of SCR firing angle, α . The measured motor current plot also confirms that motor starts with rated current. The computed and measured graphs in figure 6(b) show that the motor speed increases almost linearly and takes about 7 seconds to reach the no-load value. The computed variation of α during starting is shown in figure 6(c). It is seen that the optimum PI controller adjusts α to keep the motor current at the rated value; further, once starting is completed, α is reduced to zero due to constraints put on it. Another interesting observation is about the transient variation of electromagnetic torque depicted in figure 6(d). It is seen that the magnitude of electromagnetic torque is always positive with little ripple. The enhanced torque profile reduces shocks to shaft, bearings, gears and load. While no attempt has been made to reduce starting torque ripple, the graph in figure 6(d) suggests that rated current operation yields improved starting profile. This is particularly important because direct on-line starting causes large oscillations in the electromagnetic torque and special control techniques are needed to smoothen the torque ripple [10-11]. Thus it can be concluded that soft starting of motor optimum PI controller yields additional advantage of improved starting torque profile.

IV. CONCLUSION

This work has focused on the design and implementation of a closed loop scheme for soft-starter fed induction motor drive. The objective of the closed loop operation was to start the motor at rated current. Towards this goal, soft-starter fed induction motor drive with closed loop operation is first modeled in MATLAB. The feedback controller constants are identified for enhanced starting dynamics using Particle Swarm Optimization (PSO). The complete drive system is simulated in MATLAB first and subsequently implemented in the laboratory. A low cost PIC16F876A microcontroller was used as the feedback controller and firing pulse generator for AC voltage controller. The computed and measured results corroborate each other and validate the proposed method.

APPENDIX

SPECIFICATIONS OF THE MACHINE:

TYPE	: SQUIRREL CAGE
VOLTAGE	: 415V
RATING	: 2.2 KW
RPM	: 1435
CONNECTION	: STAR
FREQUENCY	: 50 Hz
CURRENT	: 2.7A

REFERENCES

1. R. F. McElveen, and M. K. Toney, "Starting high inertia loads," *IEEE Trans. Ind. Appl.*, vol. 37, no. 1, pp. 137–144, Jan./Feb. 2001.
2. E. P. Dick, B. K. Gupta, P. Pillai, A. Narang, T. S. Lauber, and D. K. Sharma, "Prestriking voltages associated with motor breaker closing," *IEEE Trans. Energy Convers.*, vol. 3, no. 4, pp. 855–863, Dec. 1988.
3. H. G. Tempelaar, "Determination of transient voltages caused by switching of high voltage motors," *IEEE Trans. Energy Convers.*, vol. 3, no. 4, pp. 806–814, 1988.
4. P. J. Collieran and W. E. Rogers, "Controlled Starting of AC Induction Motors," *IEEE Trans. Ind. Appl.*, IA-22, pp. 1014–1018, vol-IA-19, Dec 1983.
5. F. M. Bruce, R. J. Graefe, A. Lutz and M. D. Panlener, "Reduced-voltage starting of Squirrel-cage Induction motors," *IEEE Trans. Ind. Appl.*, vol. IA-20, pp. 46–55, Jan./Feb. 1984.
6. J. Bowerfind, and S. J. Campbell, "Application of solid-state AC motor starters in the pulp and paper industry," *IEEE Trans. Ind. Appl.*, IA-22, pp. 109–114, Jan./Feb. 1986.
7. D. Gufflet, and P. Malkin, "Solid state medium voltage contactor," *IEE Proc. B, Electr. Power Appl.*, vol. 140, no. 2, pp. 147–151, March 1993.
8. R. S. J. Iyengar and V. V. Sastry, "Fuzzy Logic based soft-starter for Induction motor drives," *Industrial applications conference.*, 1995., Thirtieth IAS Annual Meeting, IAS '95, Conference record of the IEEE 1995, pp.121-128 .
9. V. V. Sastry, M. R. Prasad, and T. V. Sivakumar, "Optimal soft starting of voltage-controller-fed IM drive based on voltage across thyristor," *IEEE Trans. Power Electron.*, vol. 12, no. 6, pp. 1041–1051, Nov. 1997.
10. 11. Cadirci, M. Ermis, E. Nalcaci, B. Ertan and M. Rahman, "A Solid state direct on line starter for medium voltage Induction motors with minimized current and torque pulsations," *IEEE Trans on Energy conversion.*, vol. 14, no. 3, pp. 402–412, Sep. 1999.

International Journal of Advanced Research in Electrical, Electronics and Instrumentation Engineering

(An ISO 3297: 2007 Certified Organization)

Vol. 5, Special Issue 8, November 2016

11. G. Zenginobuz and I. Cadirci, "Soft Starting of Large Induction Motors at Constant Current with minimized starting torque pulsations," *IEEE Trans. Industry Applications.*, vol. 37, no. 5, pp. 1334–1347, Oct 2001.
12. W. N. Li, J. G. Lu, M. S. Liu, and J. Zhao, "Design of Intelligent Soft-start Controller for Induction Motor," Proceedings of Third International Conference on Machine Learning and Cybernetics, Shanghai, 26-29 August 2004, pp. 908-912.
13. G. Zenginobuz, I. Cadirci, M. Erimis, and C. Barlak, "Performance Optimization of Induction Motors During Voltage-Controlled Soft Starting," *IEEE Trans. Energy Convers.*, vol. 19, no. 2, , pp. 278-288, June 2004.
14. Gastli and M. M. Ahmed, "ANN-based Soft starting of voltage-controlled-fed IM Drive system," *IEEE Trans on Energy conversion*, vol. 20, no. 3, pp. 497–503, Sep. 2005.
15. F. Blaabjerg, J. K. Pedersen, S. Rise, H. Hansen and A. M. Trzynadlowski, "Can soft-starters help save energy?" *IEEE Industry Applications Magazine.*, pp.56–66, sep/Oct 1997.
16. K. Sundareswaran and B. M.Jos, "Development and analysis of novel soft-starter/Energy-saver topology for delta-connected induction motors," *IEE Proc. - Electr. Power Appl.*, vol. 152, no. 4, July 2005.
17. Pinjia Zhang, Bin Lu, and Thomas G. Habetler, "A Remote and sensor less stator winding resistance estimation method for thermal protection of soft- starter- connected induction machines," *IEEE Transactions on Industrial Electronics*, vol. 55, no. 10, pp. 3611–3618, Oct. 2008.
18. Pinjia Zhang, Yi Du, Jing Dai, Thomas G.Habetler, and Bin Lu, "Impaired-cooling-condition detection using dc-signal injection for soft-starter- connected induction motors," *IEEE Transactions on Industrial Electronics*, vol. 56, no. 11, pp. 4642–4650, Nov. 2009.
19. J.Kennedy, and R.Eberhart, "Particle Swarm Optimization," in *Proc. of the IEEE Int. Conf. on Neural Networks*, Piscataway, NJ, pp. 1942-1948, 1995.
20. Chia-Feng Juang, Yu-cheng Chang and Che-meng Hsiao, "Evolving gaits of a hexapod robot by recurrent neural networks with symbiotic species-based particle swarm optimization," *IEEE Trans. Ind. Electron.*, vol. 58, pp. 3110–3119, June 2011.
21. M. A. Hassan and M. A . Abido, "competitive strategic bidding optimization in electricity markets using bilevel programming and swarm technique," *IEEE Trans. Ind. Electron.*, vol. 58, pp. 2138–2146, May 2011.
22. Rong-Jong Wai, Jeng-Deo and Kun-Lun Chunang, "Real-Time PID Control Strategy for Maglev Transportation System via Particle Swarm Optimization," *IEEE Trans. Ind. Electron.*, vol. 58, pp. 629–646, March 2011.

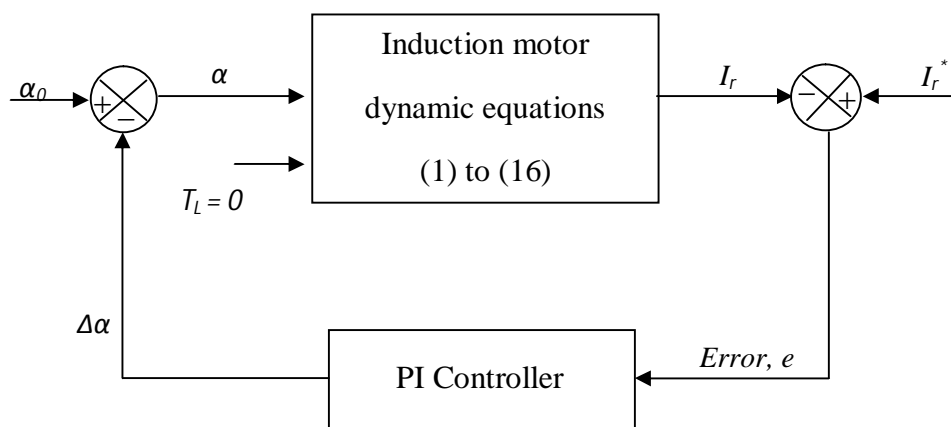


Figure 1. Block diagram of induction motor soft-starting with feedback controller.

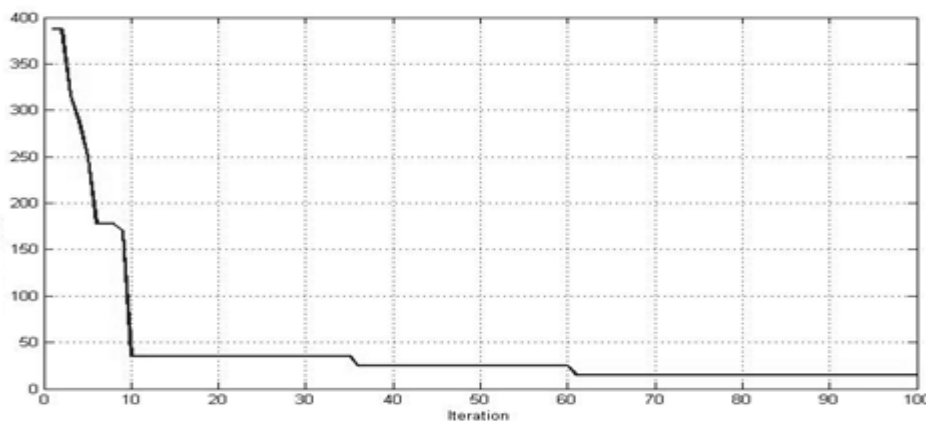


Figure 2. Convergence characteristics of the algorithm.

International Journal of Advanced Research in Electrical, Electronics and Instrumentation Engineering

(An ISO 3297: 2007 Certified Organization)

Vol. 5, Special Issue 8, November 2016

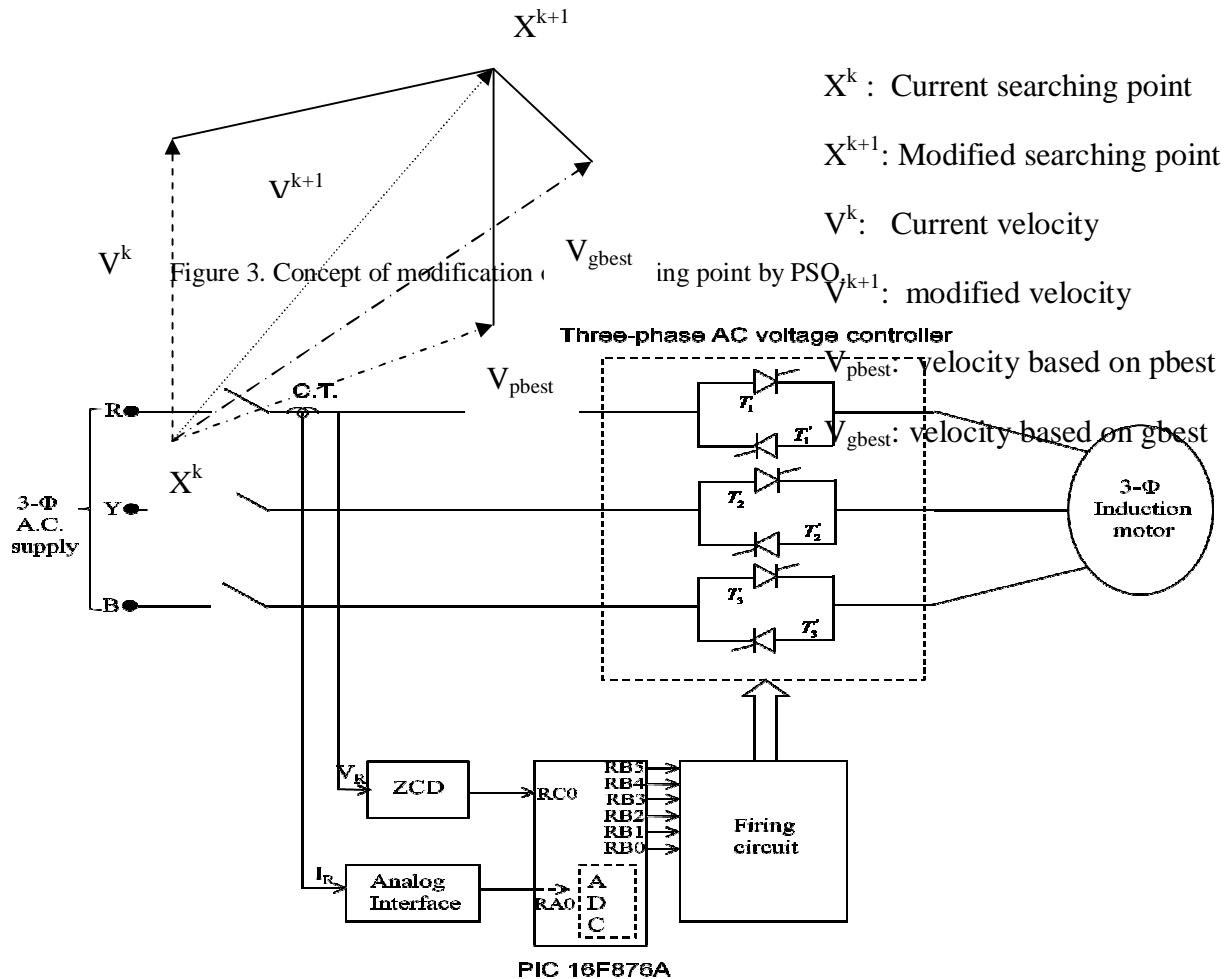
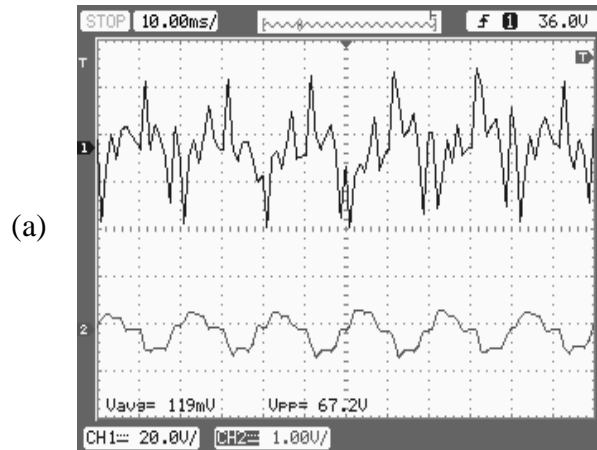
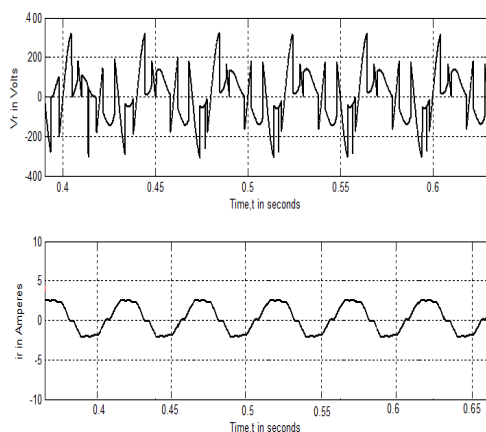


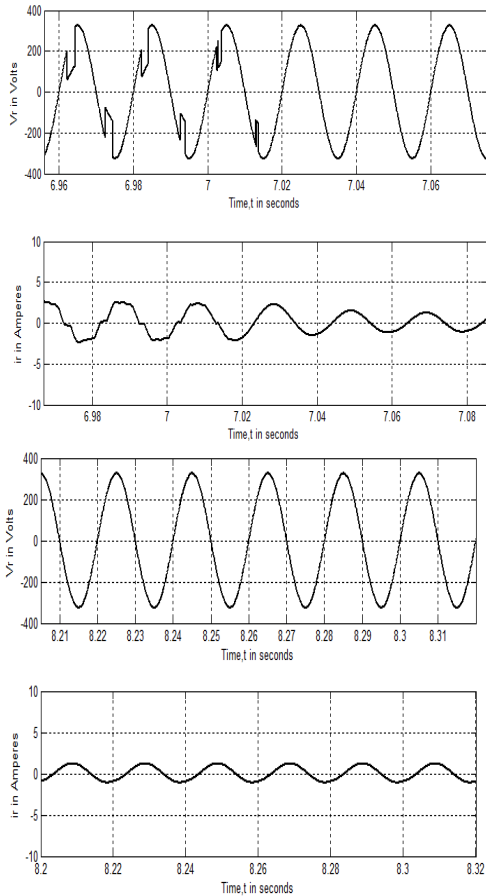
Figure 4. Experimental set up for induction motor soft-starting with feedback.



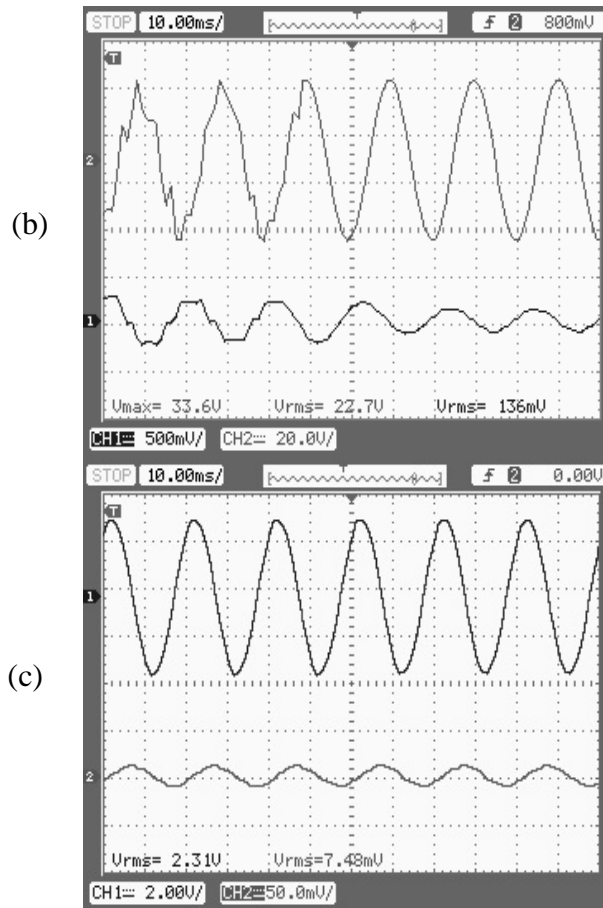
International Journal of Advanced Research in Electrical, Electronics and Instrumentation Engineering

(An ISO 3297: 2007 Certified Organization)

Vol. 5, Special Issue 8, November 2016

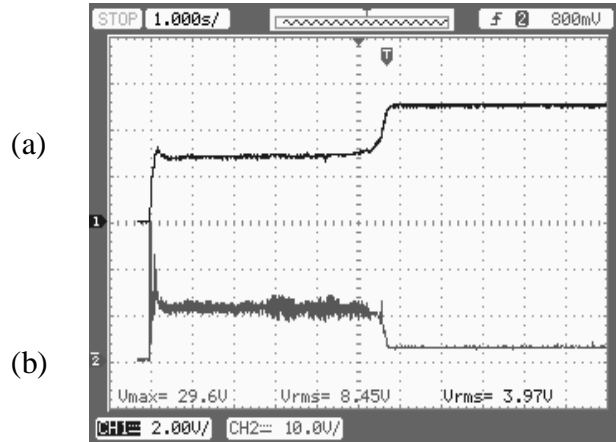
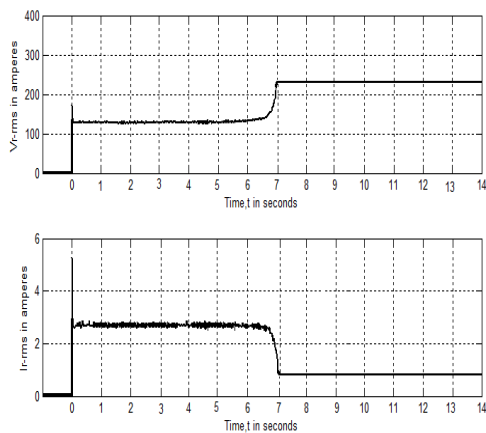


Simulated



Measured

Figure 5. Instantaneous voltage and current of the 3-phase induction motor (a) during starting (b) during the end of starting process (c) after starting process is completed.



International Journal of Advanced Research in Electrical, Electronics and Instrumentation Engineering

(An ISO 3297: 2007 Certified Organization)

Vol. 5, Special Issue 8, November 2016

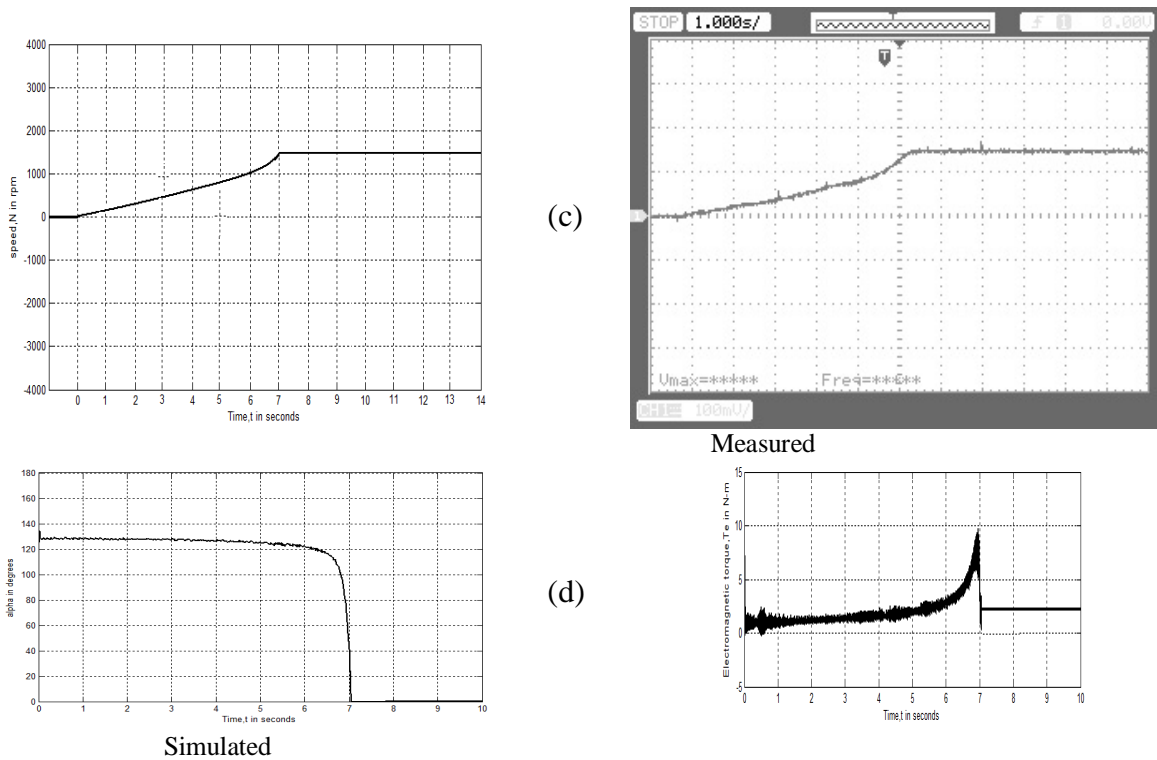


Figure 6. Instantaneous variation of (a) rms value of motor voltage (b) rms value of motor current (c) motor speed (d) SCR firing angle variation and (e) electromagnetic torque profile.